



## METHODOLOGY FOR SITE CLASSIFICATION USING STRONG GROUND MOTION DATA FROM THE 1999 CHI-CHI, TAIWAN EARTHQUAKE

Vietanh PHUNG<sup>1</sup>, Gail M. ATKINSON<sup>2</sup> and David T. LAU<sup>3</sup>

### SUMMARY

On 21 September 1999, a major earthquake of magnitude  $M_w=7.6$  occurred in central Taiwan near the city of Chi-Chi. The strong-motions of the Chi-Chi earthquake were recorded at 420 strong-motion stations in the epicentral region and around Taiwan. These valuable records greatly increase the world's existing database on near-fault strong-motion data. However, the site conditions of many of these stations in Taiwan are not known. Among the 420 strong-motion stations, the site conditions of only 87 stations are known, and these are classified into four groups (S1, S2, S3 and S4) by borehole data and some surface geology. In order to understand the characteristics of the Chi-Chi earthquake and to be able to correctly utilize the ground motion records for structural response analysis, it is important to obtain information on the site conditions of the other 333 stations. This paper presents a methodology to estimate the missing site condition information from recorded ground motion data based on the shape of the 5%-damped pseudo-acceleration spectrum of the horizontal ground motion component normalized with respect to PGA. The classification scheme is developed using the data from the 87 stations for which the site conditions are known. Records considered as weak motions are analyzed separately from the strong motion records in order to obtain insight into the significance and influences of nonlinear soil response on the results. Two different general site classes of rock and soil sites are distinguished. The site classification of rock includes hard rock, rock, and soft rock, which correspond to NEHRP site classes A, B and C, respectively. The site classification of soil includes soil, medium soil, and soft soil, which correspond to NEHRP site classes D, E and F. The results obtained from the proposed methodology correlate well with the available known site data. The proposed method has accurately classified the site conditions of 53 stations out of 61 stations with recorded PGA less than 120 gal, where linear soil behavior is expected, and the site conditions of 21 stations out of 26 stations with recorded PGA greater than 120 gal, where nonlinear soil behavior is likely to have occurred. We apply the classification method to estimate the site condition of the other 333 stations. The results indicate that 248 stations should be classified as soil and 172 stations should be classified as rock. The results obtained from this study are compared to the results obtained by Lee *et al.* [1] based on interpretation of geologic maps and geomorphologic data; our result are in agreement with theirs at 71% of the sites.

---

<sup>1</sup> Graduate Student, Department of Civil & Environmental Engineering, Carleton University, Canada

<sup>2</sup> Professor, Department of Earth Science, Carleton University, Canada

<sup>3</sup> Professor, Department of Civil & Environmental Engineering, Carleton University, Canada

Another site classification methodology based on the horizontal-to-vertical spectral ratio technique was also investigated. However this technique resulted in lower accuracy than the proposed technique based on the spectral shape. With the H/V technique, only 53 stations out of the 87 stations were classified correctly (60%).

## INTRODUCTION

### **Ground motions of 1999 Chi-Chi, Taiwan earthquake**

At 1:47 AM on 21 September 1999 an earthquake of magnitude  $M_w=7.6$  occurred in central Taiwan. The epicenter was located at  $23.78^\circ$  N and  $121.09^\circ$  E near the town of Chi-Chi. After the earthquake, the Central Weather Bureau (i.e., Lee *et al.*, [2]) successfully retrieved about 420 free-field records out of more than 650 free-field strong-motion stations. This valuable set of records increases the number of near-field strong-motion records 10-fold in the existing worldwide dataset. However, the site conditions of many of these strong-motion stations are not known or documented. In order to allow the proper use of this valuable set of strong-motion data from the Chi-Chi earthquake to characterize source and propagation effects, it is important to obtain information on the site conditions of all the strong-motion stations in Taiwan. Kou [3,4,5] has classified strong-motion sites in the Taipei, Taoyuan, Hsinchum, Miaoli and Chianan areas into four categories: S1 (hard rock), S2 (rock and hard stiff soil), which is also labeled as soft rock in California, S3 (medium stiff soil), and S4 (soft soil), by using a combination of borehole and surface geology data. However, only 87 sites out of the 420 sites that recorded the Chi-Chi earthquake were classified (7 S1-sites, 33 S2-sites, 39 S3-sites, and 8 S4-sites). Because the classifications of these 87 sites are based on directly observed site parameters (from borehole and surface observations), these sites are considered as the ‘reference sites’ with known site conditions in the present investigation. The objective of this paper is to develop a methodology for estimating the site condition of the strong-motion stations with unknown site condition. The methodology is developed with the aid of the 87 reference sites based on the characteristics of ground motions recorded at these reference stations and their observed relationships with known site conditions. Two techniques for classification of the sites are investigated, namely: (1) the spectral shape technique using the horizontal-component ground motions; and (2) the horizontal-to-vertical spectral ratio technique.

The 420 free-field ground motion records of the Chi-Chi earthquake have three components (N-S, E-W, and vertical). The 5% damped pseudo-acceleration response spectra are computed for the 420 strong-motion records for natural periods up to 5 sec, after baseline correction. The response spectra are then smoothed by using a simple 9-point weighted triangular smoothing procedure. An average horizontal component of the ground motion for each record is obtained by averaging the natural logarithms of the ground motion amplitudes.

### **Site classification**

Seed *et al.* [6,7] conducted some of the first quantitative studies of how the geological and local site conditions affect the response spectra. Following this pioneering study, the influences of the site conditions on the earthquake resistant design of structures have been incorporated in the Uniform Building Code (UBC) [8] and guidelines of the National Earthquake Hazards Reduction Program (NEHRP) [9] through the use of simplified design spectra of different shapes for different types of sites. The site classification descriptions of UBC are summarized in Table 1. It is noted that the site classification in UBC is the same as that of NEHRP. The site classification is now well established in term of shear-wave velocity. However, the practical application of using shear-wave velocity as a site classification criterion is limited due to the technical requirements and expense of obtaining shear-wave velocity measurements in the field. It is useful to develop a fast and simple methodology to estimate the site conditions based on the characteristics of the recorded ground motions. In the present study, a method is developed to classify the Taiwan strong-motion stations into different categories as defined in the design standards of UBC [8], NEHRP [9] and Japan Design Specification for Highway Bridges [10].

**Table 1.** Site classification

Site class	Site class description by 1997 UBC Provisions ( $\bar{V}_s$ is shear-wave velocity averaged over top 30 m)	Site class description in present study
A	Hard rock (typically eastern United States sites), $\bar{V}_s > 1500$ (m/s).	Rock
B	Rock, $\bar{V}_s$ is 760 to 1500 (m/s).	
C	Very dense soil and soft rock, $\bar{V}_s$ is 360 to 760 (m/s), Un-drained shear strength $S_u \geq 2000$ psf ( $S_u \geq 100$ kPa) or $N \geq 50$ blows/ft (C class is typically called a rock site in California)	
D	Stiff soils, $\bar{V}_s$ is 180 to 360 (m/s), Stiff soil with un-drained shear strength $1000 \text{ psf} \leq S_u \leq 2000 \text{ psf}$ ( $50 \text{ kPa} \leq S_u \leq 100 \text{ kPa}$ ), or $15 \leq N \leq 50$ blows/ft.	Soil
E	Soft soils, Profile with more than 10ft (3m) of soft clay defined as soil with plasticity index $PI > 20$ , moisture content $w > 40\%$ and un-drained shear strength $S_u < 1000$ psf (50kPa), or $N < 15$ blows/ft.	
F	Soils requiring site-specific evaluations. (1) 1. Soil vulnerable to potential failure or collapse under seismic loading: e.g., liquefiable soils, quick and highly sensitive clays, collapsible weakly cemented soils. (2) 2. Peats and/or highly organic clays (10ft (3m) or thicker layer). (3) 3. Very high plasticity clays: (25ft (8m) or thicker layer with plasticity index $> 75$ ). (4) 4. Very thick soft/medium stiff clays: (120ft (36m) or thicker layer).	

### SITE CLASSIFICATION ESTIMATION TECHNIQUES

The correlation between site amplification and surface geology has been the subject of many studies. One of the commonly adopted techniques to estimate site conditions is the ‘H/V technique’, based on the horizontal-to-vertical spectral ratio of earthquake records or microtremors. Nakamura [11] used the horizontal-to-vertical component spectral ratios of the ambient seismic noise, dominated by the Rayleigh waves to interpret micro-tremor measurements. Lermo and Chavez-Garcia [12] were successful in using the H/V technique for site response evaluation of three cities in Mexico using earthquake records containing S-waves and surface waves. Atkinson and Cassidy [13] were also successful in estimating the soil response of the Fraser River Delta to the Duvall and Georgia Strait earthquake by using the H/V technique. An advantage of this technique is that it does not need a reference rock site station; hence this technique is inexpensive and simple to apply. The limitation of the technique is that it lacks a detailed theoretical basis (as discussed below), and the success of the technique has been mixed. Tsuboi *et al.*

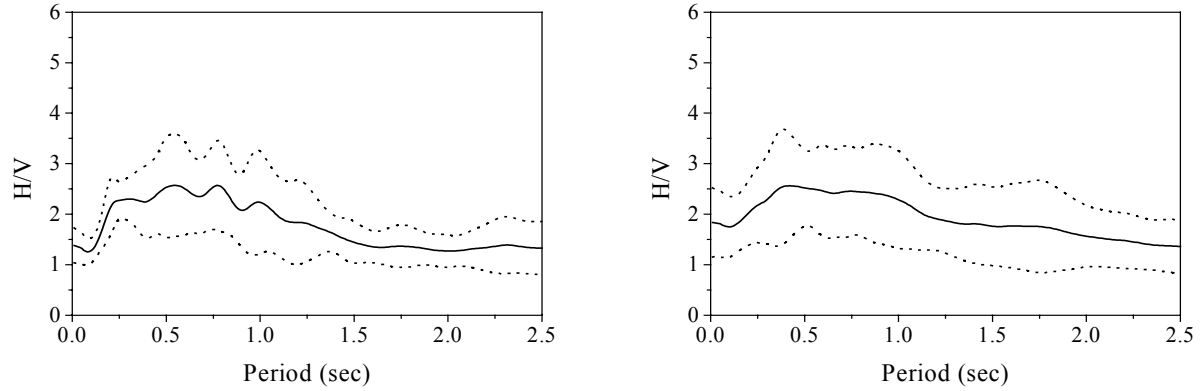
[14] found that in general the spectral peaks of the H/V ratio and actual amplifications based on borehole-to-surface measurements between 1 Hz and 4 Hz agree well, but the agreement deteriorates for higher frequencies. Bonilla *et al.* [15] have studied the borehole responses from the Garner Valley Downhole Array in Southern California and have found that the amplification obtained from the H/V spectral ratio is different from the one computed by the direct S-wave spectral ratio. Thus there are conflicting conclusions from different studies regarding the success of using the H/V ratio to estimate site responses.

Another method for site classification is the traditional technique based on the shape of response spectra obtained from earthquake records. The technique has its origins in the work of Borcherdt [16], who divided the spectrum obtained at a site of unknown site condition to that obtained at nearby reference site on competent bedrock. Seed *et al.* [6,7] investigated the differences in the shapes of normalized acceleration spectra of different site conditions and carried out statistical analysis of the results. In the following sections we investigate both the H/V technique and the spectral shape technique as potential discriminants of site condition for the strong-motion stations in Taiwan.

### **Horizontal-to-vertical spectral ratio technique**

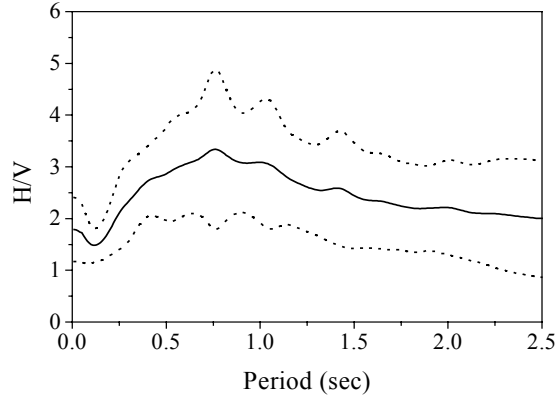
The reliability of the H/V technique in predicting the amplification effects of the surface soil layer is often questioned. This is because the basic principle of the H/V technique is largely qualitative. For a soft layer overlying a half-space, or for a velocity gradient, the horizontal component of the wave amplitude ( $S_H$ ) is amplified by the soft soil layer as the wave propagates to the surface. There may also be amplification and attenuation of the vertical component, which tends to be dominated by  $S_V$  except at very high frequencies (i.e., Beresnev *et al.*, [17]). However, the amplification of  $S_V$  is counterbalanced by the effects of refracting the ray path toward the vertical direction. Consequently, the net amplification effects of the vertical component are relatively small compared to those of the horizontal component, and may be considered negligible. Thus the H/V ratio is an estimate of site amplification, and may be useful in determining site condition. This view is supported by the studies by Nakamura [11], Lermo and Chavez-Garcia [12], and Atkinson and Cassidy [13], but not supported by the study of Bonilla *et al.* [15].

Here, amplitude and frequency characteristics of the horizontal-to-vertical spectral ratios are used to classify the site conditions of strong-motion stations in Taiwan. The H/V spectral ratio is computed for periods up to 2.5 sec for the 87 strong-motion stations where the site conditions are known. Figure 1 shows the mean horizontal-to-vertical spectral ratio and its standard deviation ( $\sigma$ ) for four site groups based on NEHRP site classes: 1 = A/B (7 strong ground motion records); 2 = C (33 strong ground motion records); 3 = D (39 strong ground motion records); and 4 = E/F (8 strong ground motion records). The peak of the mean H/V ratio increases in amplitude and predominant period from rock sites to the medium-to-soft soil sites. Although the average H/V is different for each category plotted, there is considerable overlap of the H/V amongst classes when one considers the scatter as indicated by the  $H/V \pm \sigma$ . This scatter is an important constraint in developing a successful site class discriminant. It is observed that the peak H/V spectral ratios are 2.57, 2.56, 3.33, and 3.76 with predominant period at 0.55 sec, 0.4 sec, 0.75 sec, and 1.0 sec for NEHRP classes A/B, C, D, and E/F, respectively.

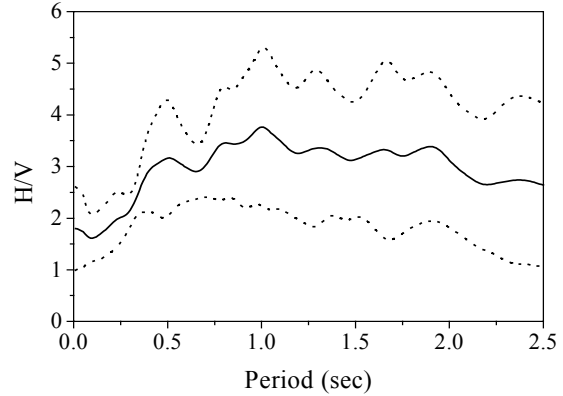


a) A and B (S1) sites.

b) C (S2) sites.



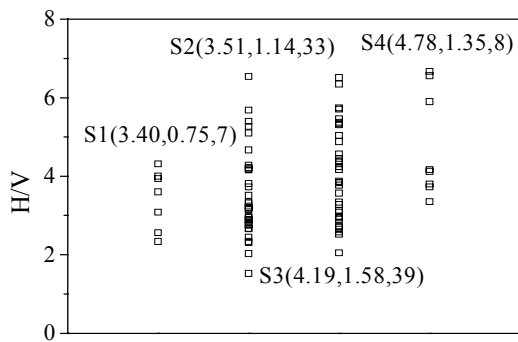
c) D (S3) sites.



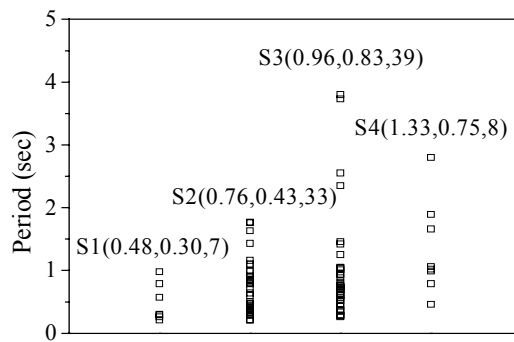
d) E and F (S4) sites.

**Figure 1.** Average H/V spectral ratio for A/B (S1), C (S2), D (S3) and E/F (S4) sites. Dotted lines indicate  $\pm$  one standard deviation level.

Figure 2 shows the individual peak H/V and predominant period of the H/V spectra for S1 (A and B), S2 (C), S3 (D), and S4 (E and F) site classes. There are no pronounced differences in peak H/V and predominant period of H/V spectra between rock sites and soil sites, although the average H/V and the predominant period of average H/V spectra for soil sites (D, E and F) are larger than those for the rock sites (A, B and C).



a) Peak H/V.



b) Predominant period of H/V.

**Figure 2.** Peak H/V and predominant period of H/V spectra for A and B (S1), C (S2), D (S3) and E and F (S4) sites. Notations at each column give: site class, mean, standard deviation and number of records.

Figure 3 shows the individual H/V values for hard rock (A and B), soft rock (C), stiff soil (D) and medium-to-soft soil (E and F) for periods  $T=0.1$  sec, 0.2 sec, 0.5 sec, 1.0 sec, 1.5 sec and 2.5 sec. For the period range from 0.1 to 2.5 sec, the H/V of soil sites and that of rock sites are overlapping. The degree of variability of H/V within each site class plays an important role in developing a site classification estimation scheme.

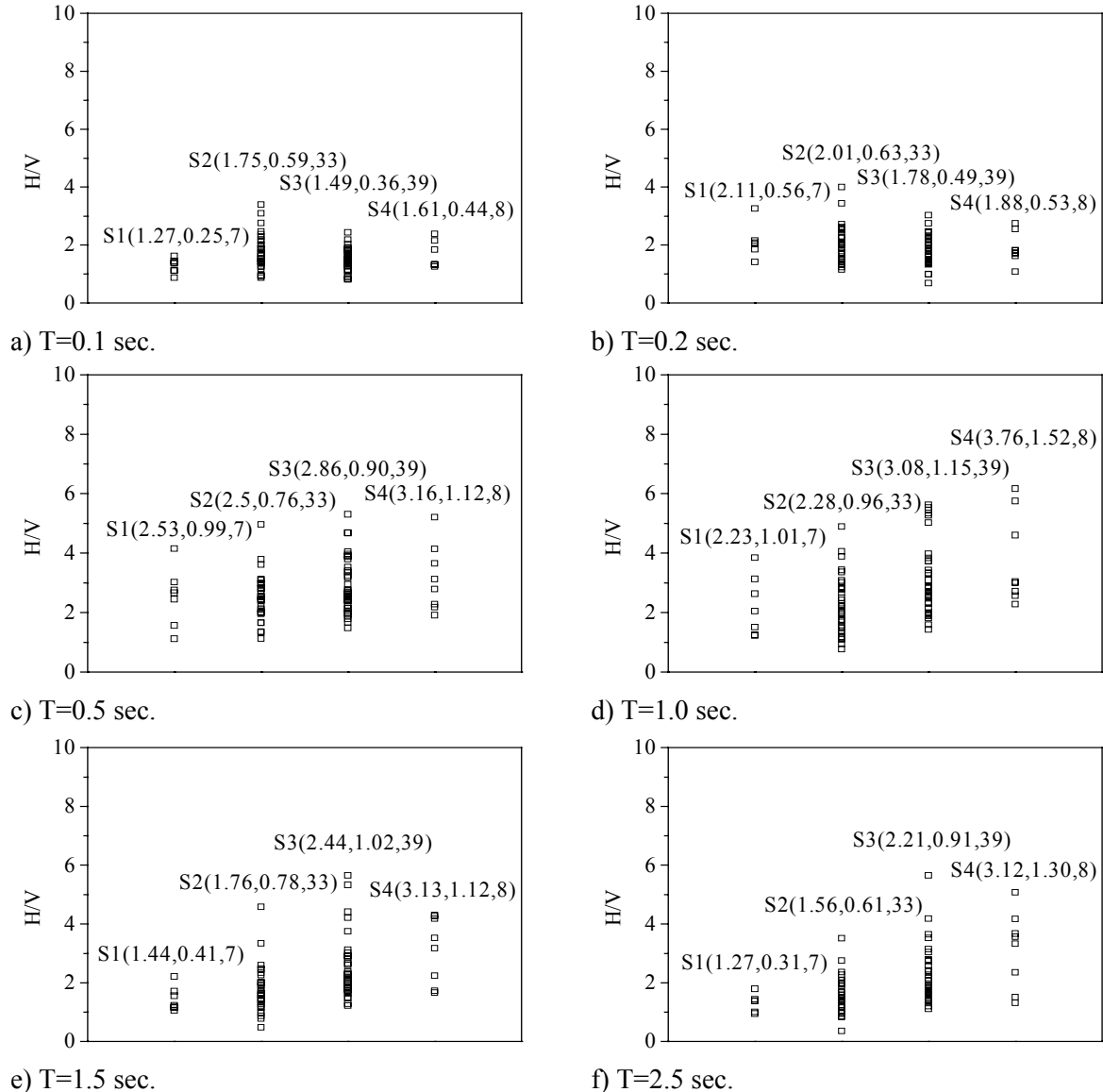


**Figure 3.** H/V spectral ratio for different periods 0.1, 0.2, 0.5, 1.0, 1.5 and 2.5 sec. Notations at the top of each column give: site class, mean, standard deviation and number of records.

Some possible discriminants for site classification estimation based on the H/V technique have been examined; these included the use of peak H/V value, predominant period of H/V spectra, and values of H/V at specific periods. The use of the peak H/V value and its period provides the most statistically significant discriminant among these alternatives. The trial site classification estimation method based on H/V works as follows. If the peak H/V  $< 2$  then the site may be classified as rock, while if the peak H/V  $\geq 5$  then the site may be classified as soil. For sites with  $2 \leq H/V < 5$ , the period at which the peak H/V occurs is used as a discriminant. If predominant period is larger than 0.6 sec, the site is classified as soil and if predominant period is smaller than 0.6 sec, the site is classified as rock. However, because of the

considerable overlap of H/V between rock and soil sites, the accuracy of the method is only 61% (53 stations out of the 87 stations are classified correctly).

### Response spectral shape technique

The use of response spectral shape as a characterization tool of soil response has its origins in the work of Borchardt [16], who used the ratio of spectra on soil sites to those on nearby rock sites to estimate the response of the soil sites. The underlying assumption is that the rock sites are free of amplification, and thus the ratio of the soil to rock spectra provided the shape and amplitude of the site response. Seed *et al.* [6,7] used normalized acceleration spectra to characterize the spectral shapes of several different site conditions. In the Japan Specification for Highway Bridges [10], Part 5 Seismic Design, the values for predominant periods are approximately given as  $T_g < 0.2$  sec for hard rock and rock sites (NEHRP site type A and B),  $0.2 \text{ sec} \leq T_g < 0.6$  sec for rock and stiff soil sites (NEHRP site type C and D), and  $T_g \geq 0.6$  sec for soft to medium soil sites (NEHRP site type E and F). Recently, Borchardt [18] proposed a general methodology for developing estimates of site-dependent response spectra for design based on the use of extensive borehole geologic, geotechnical and shear-wave velocity data. Thus the use of the response spectral shape, in various forms, has a long history as a site condition discriminant.

In this section, a method is developed to estimate the site condition for stations in Taiwan by using the spectral shape of the normalized acceleration spectra of the horizontal ground motion component. Normalized acceleration spectra are obtained as the response spectrum divided by the peak ground acceleration (PGA). Figure 4 shows the spectral shapes for NEHRP site classes (A/B), C, D and E/F, respectively, as obtained from the Chi-Chi data of the 87 sites with known site conditions.

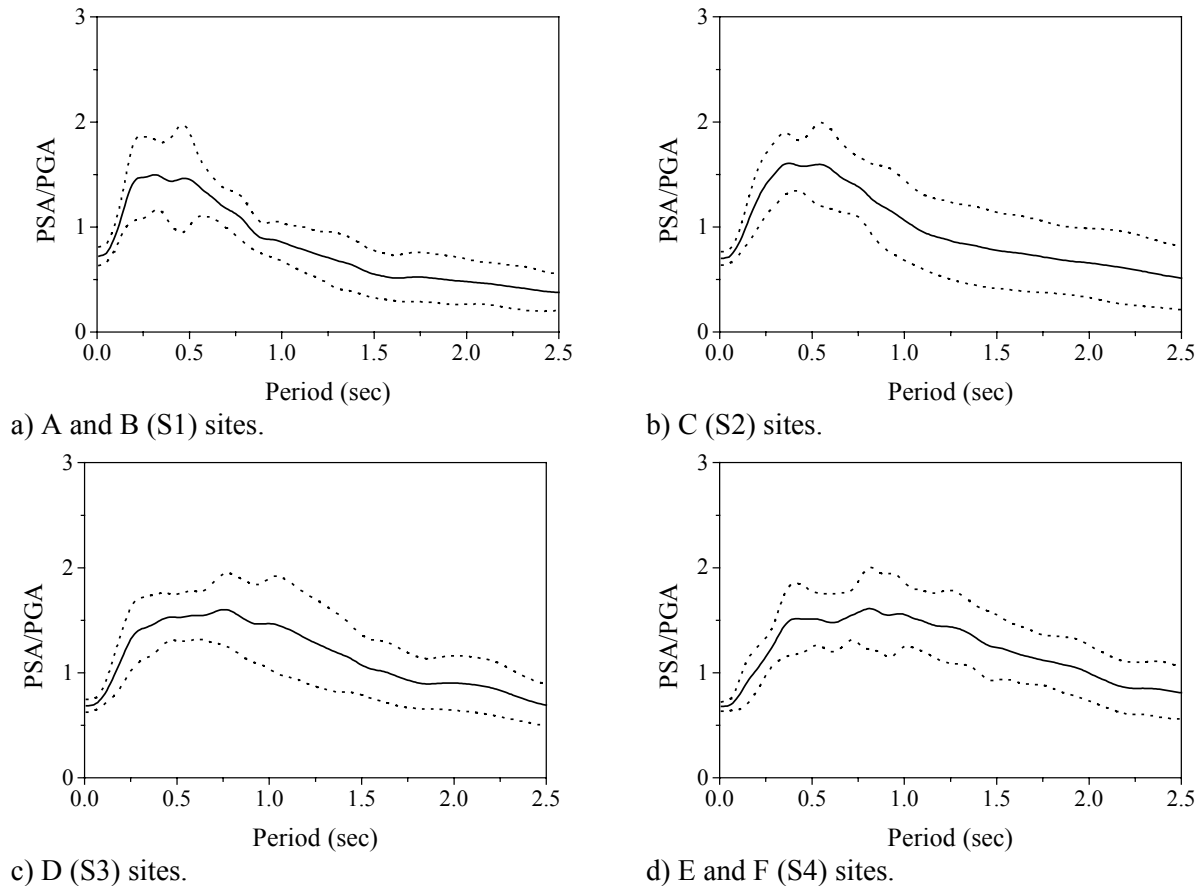


**Figure 4.** Average normalized spectra of horizontal strong-motion component for A/B, C, D and E/F sites. Dotted lines indicate  $\pm$  one standard deviation level.

The predominant periods of the normalized acceleration spectra for NEHRP site class A/B (S1), C, D, and E/F (S4) are approximately 0.3 sec, 0.35 sec, 0.75 sec and 1.0 sec, respectively. The normalized acceleration spectra for all site classes are very similar in the range of periods from 0.3 to 0.6 sec. In the range of periods from 0.6 sec to 1.0 sec, the normalized acceleration spectra for rock sites (A, B and C) decline quite dramatically (40% reduction in amplitude) with increasing period, while the amplitudes of the normalized acceleration spectra for soil sites (D, E and F) decrease more gently as period increases. This characteristic of the normalized acceleration spectra is used as a discriminant for site classification. To utilize this observation, the shape of the normalized acceleration spectra is characterized by the shape ratio (SR), which is defined as the amplitude of the normalized acceleration spectra at T to that at its dominant (peak) period:

$$SR(T) = (PSA(T)/PGA) / (PSA(T_g)/PGA)$$

$$SR(T) = PSA(T) / PSA(T_g) \quad (2)$$

where T is period in seconds and  $T_g$  is dominant period in seconds.

The shape ratio SR at 1.0 sec and the predominant period of the spectra of the horizontal ground motion component are shown individually for each station in Figure 5. The mean of the SR at 1.0 sec and predominant period for soil sites are considerably larger than those for rock sites; however there is an overlap between soil sites and rock sites. The possibility that this overlap may be partly due to nonlinear soil response is investigated later.

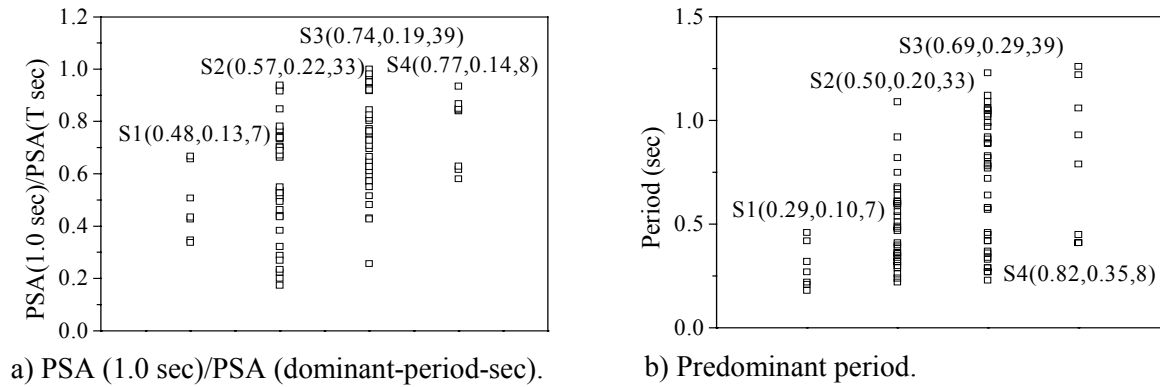
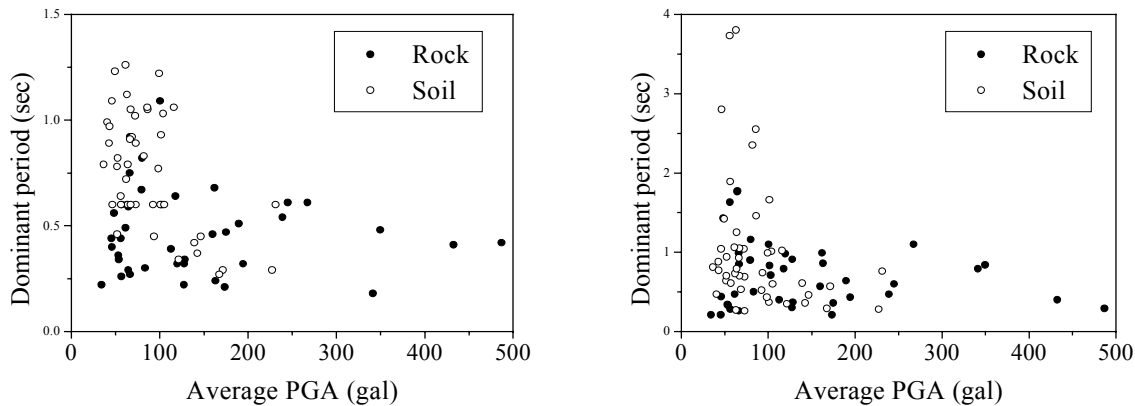


**Figure 5.** PSA (1.0 sec)/PSA (dominant-period-sec) and predominant period of the spectra of horizontal ground motion component for A and B (S1), C (S2), D (S3) and E and F (S4) sites. Notations at each column give: site class, mean, standard deviation and number of records.

Based just on the use of predominant period of the spectra shape, a simple classification procedure is developed as follows: if a site has a predominant period  $\geq 0.6$  sec it may be classified as soil (NEHRP site class D, E and F), while sites with predominant period  $< 0.6$  sec may be classified as rock (NEHRP site class A, B and C). This technique accurately classifies 68 stations out of 87 stations (78% accuracy). As noted earlier, there is an overlap in predominant period of normalized acceleration spectra between rock and soil sites. There are a significant number of soil sites associated with large PGA that have a predominant period  $< 0.6$  sec. At these sites, nonlinear soil response due to strong shaking may have some impact on the spectral shape of the normalized acceleration spectra. This possibility is investigated in the next section, with an aim to improving the classification scheme to account for such effects.

## Effects of ground motion intensity

Strong ground motion can cause soil to behave nonlinearly. Evidence of nonlinear behavior is usually observed when the PGA exceeds a threshold of 100 to 200 gal (Beresnev and Wen, [19]). Nonlinear soil effects include an increase in damping and reduction in resonant frequencies as ground motion intensity increases. Nonlinear soil effect during large earthquakes have been the subject of many studies since the pioneering work of Seed *et al.* [6,7], in which soil nonlinearity was recognized to play an important role. However, for many years these effects were ignored because of the lack of data from strong-motion observations. The situation has changed due to evidence from recent observations from the 1985 Michoacan, Mexico (Singh *et al.*, [20]), the 1989 Loma Prieta, (Chin and Aki, [21]), and the 1994 Northridge California, earthquakes (Beresnev *et al.*, [22]). Other evidence of nonlinear site response during strong ground motion has been provided in many studies as reviewed by Beresnev *et al.* [19]. Yu *et al.* [23] compared the Fourier spectral ratio (of soil motion divided by rock motion) obtained from strong-motion to that from weak motion and found characteristics of nonlinear soil behavior can be separated into three frequency bands. In the lowest frequency band, the soil amplification is not affected by nonlinearity. In the central frequency band, soil amplification is reduced by nonlinearity. At high frequencies, the amplification is actually higher for nonlinear than for linear soil response. The transition frequencies between these ranges depend on the soil properties, the thickness of sediments, and the amplitude and frequency content of the input signal. It is likely that the soil at some of the Taiwan sites behaved nonlinearly during the Chi-Chi earthquake and this may affect the site classification results. In this section the relationship of the shape ratio, the H/V ratio and predominant period to the ground motion intensity is explored.



a) Spectral shape technique: effect of intensity on predominant period

b) H/V technique: effect of intensity on peak period of H/V ratio

**Figure 6.** Effects of ground motion intensity on the predominant period of normalized acceleration spectra and that of H/V spectra.

Figure 6 shows the predominant period of the normalized acceleration spectra and that of H/V spectra as a function of the PGA of the record. Figure 6 (a) shows that the predominant period of normalized acceleration spectra for soil sites (D, E and F) are larger than those for rock sites (A, B and C) when  $PGA < 100$  gal. When  $PGA \geq 100$  gal, nonlinear soil response may have occurred, reducing the dominant period of the soil. Aki and Chin [21] investigated the 1989 Loma Prieta earthquake and reported that the threshold PGA for nonlinear soil response is 0.1 g, while Wen *et al.* [24,25] investigated the nonlinear site amplification at two downhole strong ground motion arrays in Taiwan and reported the nonlinear threshold as 0.15 g. Figure 6 (a) appears to support a nonlinear threshold in the range of 0.1 to 0.15 g, although the data are sparse. Nonlinear effects are also apparent in Figure 6 (b), although not as clearly as in Figure 6 (a). It should also be noted that previous studies using the H/V ratio with micro tremor

measurements by Nakamura [11], aftershock measurement by Field and Jacobs [26] or earthquake recordings by Lermo and Chavez-Garcia [12], have been based on ground motions in the linear range.

Based on observations from Figure 6 and results from the studies mentioned earlier, a PGA threshold of 120 gal for the onset of nonlinearity is adopted for the purposes of this study. There are 98 stations out of 420 stations that recorded the Chi-Chi earthquake where the  $PGA \geq 120$  gal, and which thus may have responded nonlinearly. In order to compare the spectral shape of high intensity ground motion and that of low intensity ground motion, the H/V spectra and the PSA/PGA spectra for rock and soil sites with  $PGA \geq 120$  gal are plotted in Figure 7. Figure 7 also shows the spectra of the records having  $PGA < 120$  gal for comparison. It is observed that as periods increase from 2.5 sec to 5 sec, the differences between the linear soil response (solid line) and nonlinear soil response (dashed line) become smaller. In both the linear and nonlinear cases, the long-period amplitude of the normalized acceleration spectra is greater for soil sites than for rock sites. Thus, it is possible to use the long-period normalized acceleration spectra as a discriminant for site classification where nonlinear soil response is suspected to take place.

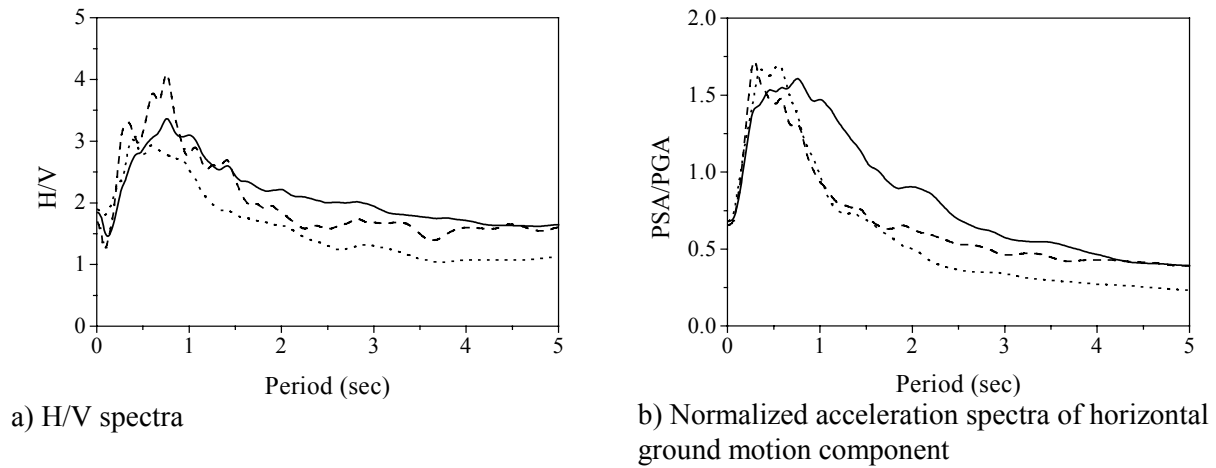


**Figure 7.** Average H/V spectra and horizontal ground motion component spectra for stations with  $PGA \geq 120$  gal (solid line for soil sites with  $PGA < 120$  gal, dashed line for soil sites with  $PGA \geq 120$  gal, dotted line for rock sites)

Figure 7 (b) shows that the predominant period of normalized acceleration spectra for the soil sites is significantly reduced at high PGA levels due to nonlinear soil response. However, the long-period end of the normalized acceleration spectra ( $> 4$  sec) does not change for high PGA. These observations agree with the findings of Yu *et al.* [23]: the predominant periods of the normalized acceleration spectra of the Chi-Chi data occur in the central-frequency band affected by nonlinear soil behavior, whereas the normalized acceleration spectra at long period region are not affected by nonlinear soil behavior. Since the normalized acceleration spectra at long periods ( $\geq 2.5$  sec) may be affected by noise and other factors, the normalized acceleration spectral ordinates at 2.5 sec is used as a discriminant to classify the sites where  $PGA \geq 120$  gal, as described below.

### Site classification methodology

Based on the observations and statistical results presented in the previous sections, and considering nonlinear soil response, a site classification method is proposed as follows.

- (1) The stations are divided into two categories based on PGA: stations with  $PGA \geq 120$  gal (strong-motion intensity) and  $PGA < 120$  gal (weak-to-medium motion intensity).
- (2) The 5% damped pseudo-acceleration spectrum is computed using the average horizontal component of ground motion, and the spectra are normalized with respect to PGA.

- (3) For stations with  $PGA < 120$  gal, the predominant period of the spectra of the horizontal ground motion component is used as the discriminant for site classification. The site is classified as rock if predominant period  $< 0.6$  sec. The site is classified as soil if predominant period  $\geq 0.6$  sec. (Note: if the spectrum has a plateau extending over a period range that exceeds 0.6 sec, it is classified as soil even if the period at which the maximum amplitude occurs is actually below 0.6 sec).
- (4) For stations associated with  $PGA \geq 120$  gal,  $PSA(2.5 \text{ sec})/PGA$  is used as a discriminant. If  $PSA(2.5 \text{ sec})/PGA \geq 0.5$  then the site is classified as soil. If  $PSA(2.5 \text{ sec})/PGA < 0.5$  then the site is classified as rock.

By using the proposed site classification estimation methodology given above, 53 stations out of 61 stations (87%) with  $PGA < 120$  gal are accurately classified, and 21 stations out of 26 stations (80%) with  $PGA \geq 120$  gal are accurately classified. Among the 54 sites classified as soil by this technique, one site is S1 (A and B), 9 sites are S2 (C), 36 sites are S3 (D), and 8 sites are S4 (E and F), according to Kou [3,4,5]. Thus the proposed methodology has misclassified one A/B class and 9 C class sites as soil. Among the 33 sites classified as rock by this technique, 3 sites are S3 (D), 24 sites are S2 (C), and 6 sites are S1 (A and B) (Kou [3,4,5]). Thus the proposed methodology has misclassified 3 class D sites as rock sites. It is noted that site classification is somewhat more accurate for sites of linear soil response than for those of nonlinear soil response.

The classification methodology based on spectral shape has a similar level of accuracy to that proposed by Lee *et al.* [1] overall, but the classifications by the two methodologies can disagree. Lee *et al.* [1] classified the sites into four different NEHRP classes (B, C, D, E) based primarily on interpretation of geologic maps and geomorphology data. The response spectral shape method and the horizontal-to-vertical spectral ratio were evaluated for each site by Lee *et al.* [1], but no statistics on how these parameters were used as site discriminants was provided in their paper. About 77% of the sites classified by Lee *et al.* [1] agree with site classifications obtained from the proposed methodology here. Among the 54 sites classified as soil here, 28 sites are classified as E class, 20 sites are classified as D class, and 4 sites are classified as C class by Lee *et al.* [1], with 2 sites of no classification. Among the 33 sites classified as rock here, one site is classified as E class, 15 sites are classified as D class, 15 sites are classified as C class, and 2 sites are classified as B class by Lee *et al.* [1]. There is a considerable overlap between the D class sites of Lee *et al.* and the rock sites obtained from this study. Comparing the classifications of Lee *et al.* [1] with those by Kou [3,4,5], the results by Lee *et al.* [1] match the classifications by Kou [3,4,5] (i.e., A/B=S1, C=S2, D=S3, E/F=S4) in only 48% of the cases. However, the comparison shows that soil sites (S3, S4 = D, E and F) are correctly distinguished from rock sites (S1, S2 = A, B and C) by Lee *et al.* [1] in 83% of the cases. The discrepancies in distinguishing between rock sites and soil sites involve sites classified as class D by Lee *et al.* [1] that are actually S2 (C) according to Kou [3,4,5]. The results (Figures 4 and 5) indicate that the amplification characteristics of the S2 sites are very similar to those of the S1 sites (rock), while Lee *et al.* [1] classified many of the S2 sites as soil. The rock classifications obtained from this study agree very closely with the known S1 and S2 classifications by Kou [3,4,5]. Thus the proposed site classification methodology based on predominant period may be more diagnostic of rock sites than the classifications by Lee *et al.* [1] based on map interpretation. It should be acknowledged that uncertainty in classification exists with both the proposed methodology and that of Lee *et al.* [1]. The differences between two classifications provide some measures of this uncertainty. Appendix A compares the site classifications from both this study and the Lee *et al.* [1] study with the known conditions according to Kou [3,4,5].

We applied our classification method to the 333 strong-motion sites in Taiwan with unknown site conditions. Results are listed in Appendix B. We classify 248 sites as soil. Of these, Lee *et al.* [1] classified 15 sites as B class, 18 sites as C class, 132 sites as D class, 79 sites as E class and 4 sites with no classification. Approximately 13% of the sites that are classified as soil sites here are considered as

rock sites (A, B and C) by Lee *et al.* [1]. There are 172 sites classified as rock by our method. Of these Lee *et al.* [1] classified 35 sites as B class, 42 sites as C class, 69 sites as D class, 14 sites as E class and 12 sites with no classification. Approximately 48% of the sites classified as rock sites in this study are identified as soil sites (D, E and F) by Lee *et al.* [1]. Overall, the results from this study agree with those of Lee *et al.* [1] at 71% of the sites. These discrepancies suggest there is still significant uncertainty in site classification for the strong-motion sites in Taiwan.

## CONCLUSIONS

Site classification techniques are reviewed and applied to estimate the site condition for strong-motion sites in Taiwan that recorded the Chi Chi earthquake. For sites that responded linearly ( $PGA < 120$  gal), the predominant period can be used as a discriminant to distinguish soil sites from rock sites. The site is classified as rock if predominant period  $< 0.6$  sec. The site is classified as soil if predominant period  $\geq 0.6$  sec. For sites that behaved nonlinearly, the spectral shape at long periods needs also to be considered. The comparison of site classification results with known soil conditions shows that 87% of the stations where linear soil response occurred during the Chi-Chi earthquake and 80% of the stations where nonlinear soil response occurred are classified correctly. It is therefore concluded that the proposed spectral shape technique is a good approach for classification of site conditions.

Observed spectral shape characteristics depend not only on site conditions, but also on earthquake magnitude and distance. Thus discriminants of site condition based on shape should be re-examined using local earthquake data before application to other earthquake regions. However, the predominant period tends to be dominated by the influence of site amplification, as evidenced by results and observation reported extensively in the literature and practical applications of similar techniques (e.g., Japan Specifications for Highway Bridges, 1996). Similar procedures may be developed to estimate the soil conditions of seismograph stations with unknown site conditions elsewhere, but would require statistical analyses to evaluate spectral shape characteristics in those regions.

## REFERENCES

1. Lee C.T., Cheng C.H., Liao C.W., Tsai Y.B. (2001) "Site Classification of Taiwan Free-Field Strong-Motion Stations." *Bull. Seism. Soc. Am.*, **91**, 221-243.
2. Lee W.H.K., Shin T.C., Kuo K.W., and Chen K.C. (1999) "CWB free-field strong-motion data from the 921 Chi-Chi earthquake." Volume 1: Digital acceleration files on CD-ROM. Seismology Center, Central Weather Bureau, Taipei, Taiwan.
3. Kou, K.W. (1992) "The geological character of the CWB Strong-motion Network – Taipei area." *Central Weather Bureau*, 77 pp. (in Chinese)
4. Kou, K.W. (1993) "The geological character of the CWB Strong-motion Network – Taoyuan Hsinchu, and Miaoli area." *Central Weather Bureau*, 76 pp. (in Chinese)
5. Kou, K.W. (1994). "The geological character of the CWB Strong-motion Network – Chianan area." *Central Weather Bureau*, 98 pp. (in Chinese)
6. Seed, H. B. and Idiss M. (1969) "The influence of soil conditions on ground motion during earthquake." *J. Soil Mechn. Foundations Div. ASCE* **94**, 93-137
7. Seed, H. B., Ugas, C., and Lysmer, J. (1976) "Site-dependent spectra for earthquake-resistant design." *Bull. Seism. Soc. Am.*, **66**, 221-243.
8. International Council of Building Officials (ICBO), 1997, *Uniform Building Code*, Whittier, CA.

9. Building Seismic Safety Council (BSSC), 1998, 1997 Edition NEHRP Recommended Provisions for Seismic Regulations for New Buildings and Other Structures, *FEMA302/303*, developed for the Federal Emergency Management Agency, Washington, DC, 337 pp.
10. Japan Specification for highway bridges (1996) Part V, *Earthquake Resistant Design*
11. Nakamura, Y. (1989) "A method for dynamic characteristics estimation of subsurface using micro-tremor on the ground surface." *QT.RTR1*, **30**, 25-33.
12. Lermo, J., and Chavez-Garcia, F. (1994) "Are micro-tremors useful in site response evaluation." *Bull. Seism. Soc. Am.*, **84**, 1350-1364.
13. Atkinson, G. and Cassidy, J. (2000) "Integrated use of Seismograph and Strong -Motion Data to Determine Soil Amplification: Response of the Fraser River Delta to the Duvall and Georgia Strait Earthquakes." *Bull. Seism. Soc. Am.*, **90**, 1028-1040.
14. Tsuboi, S., Saito, M., and Ishihara, Y. (2001) "Verification of Horizontal-to-Vertical spectral ratio technique for estimation of site response using borehole seismographs." *Bull. Seism. Soc. Am.*, **91**, 499-510.
15. Luis Fabian Bonilla, Jamison H. Steidl, Jean-Christophe Gariel, and Ralph J. Archuleta (2002) "Borehole response studies at the Garner Valley Downhole Array, Southern California." *Bull. Seism. Soc. Am.*, **92**, 3165-3179.
16. Borcherdt, RD (1970) "Effects of local geology on ground motion near San Francisco Bay." *Bull. Seism. Soc. Am.*, **60**, 29 - 61.
17. Beresnev, Igor A., Nightengale, Amber M., Silva, Walter J. (2002) "Properties of Vertical Ground Motions." *Bull. Seism. Soc. Am.*, **92**, 3152-3164.
18. Borcherdt R.D. (1995) "Site-dependent spectra for earthquake-resistant design." *Bull. Seism. Soc. Am.*, **66**, 221-243.
19. Beresnev, Igor A., Wen, Kuo-Liang (1996) "Nonlinear Soil Response – A reality?" *Bull. Seism. Soc. Am.*, **86**, 1964-1978.
20. Singh, SK; Mena, E; Castro, R (1988) "Some aspects of source characteristics of the 19 September 1985 Michoacan earthquake and ground motion amplification in and near Mexico City from strong motion data." *Bull. Seism. Soc. Am.*, **78**, 451 - 477.
21. Byau-Heng Chin and Keiiti Aki (1991) "Simultaneous study of source, path, and site effects on strong-motion ground during the 1989 Loma Prieta earthquake: A preliminary result on pervasive nonlinear site effects." *Bull. Seism. Soc. Am.*, **81**, 1859-1884.
22. Beresnev, I., G. Atkinson, P. Johnson and E. Field (1998). "Stochastic finite-fault modeling of ground motions from the 1994 Northridge, California earthquake. II. Widespread nonlinear response at soil sites." *Bull. Seism. Soc. Am.*, **88**, 1402-1410.
23. Yu, G., J.G. Anderson, and R. Siddharthan (1992) "On the Characteristics of Nonlinear Soil Response." *Bull. Seism. Soc. Am.*, **83**, 218-244.
24. Wen, K.L. (1994). "Nonlinear Soil Response in Ground Motion." *Earthquake Eng. Struct. Dyn.* **23**, 599-608
25. Wen, K.L., Beresnev I., and Yeh, Y.T. (1995) "Investigation of nonlinear site amplification at two Downhole strong ground motion arrays in Taiwan." *Earthquake Eng. Struct. Dyn.* **24**, 313-324
26. Field, E. H.; Clement, A. C.; Jacob, K. H.; Aharonian, V.; Hough, S. E.; Friberg, P. A.; Babaian, T. O.; Karapetian, S. S.; Hovanessian, S. M. and Abramian, H. A. (1995) "Earthquake Site Response Study in Giumri (formerly Leninakan), Armenia Using Ambient Noise Observations." *Bull. Seism. Soc. Am.*, **85**, 349 - 353.

**Appendix A:** Site classification for 87 stations with known soil conditions

Stn. name	Estimated site by			
	Kou [3,4,5]	Lee [1]	RSS	HVSR
TCU047	S1	C	R	S
TCU046	S1	B	R	R
TCU045	S1	C	R	R
TCU042	S3	D	R	R
TCU040	S3	E	S	S
TCU039	S2	C	S	S
TCU038	S3	D	S	R
TCU036	S2	D	S	S
TCU034	S1	C	R	R
TCU033	S3	D	S	S
TCU031	S2	D	S	S
TCU029	S1	C	R	R
TCU026	S2	D	S	S
TCU025	S1	B	R	R
TCU018	S2	C	R	S
TCU017	S2	?	S	S
TCU015	S1	C	S	S
TCU014	S2	D	R	S
TCU011	S3	D	S	S
TCU010	S2	C	S	S
TCU009	S2	D	S	S
TCU008	S2	C	S	S
TCU007	S2	D	R	S
TCU006	S3	D	S	S
TCU003	S3	D	S	S
TAP028	S3	D	S	S
TAP026	S3	E	S	S
TAP024	S3	D	S	R
TAP021	S3	E	S	S
TAP020	S3	E	S	S
TAP017	S3	E	S	S
TAP014	S3	E	S	S
TAP013	S3	E	S	S
TAP012	S3	E	S	S
TAP010	S4	E	S	S
TAP008	S3	E	S	S
TAP007	S3	E	S	S
TAP006	S3	E	S	S
TAP005	S4	E	S	S
TAP003	S4	E	S	S
CHY100	S3	D	S	R
CHY099	S3	D	S	S
CHY096	S3	D	S	S
CHY090	S3	E	S	R
CHY088	S2	D	R	S
CHY087	S2	C	R	R

Stn. name	Estimated site by			
	Kou [3,4,5]	Lee [1]	RSS	HVSR
CHY081	S2	C	R	S
CHY079	S2	C	R	R
CHY078	S3	D	S	S
CHY074	S2	C	R	S
CHY071	S4	E	S	S
CHY070	S3	D	S	S
CHY069	S3	E	S	R
CHY067	S3	E	S	S
CHY066	S3	E	S	S
CHY065	S2	D	R	S
CHY063	S2	D	R	R
CHY062	S2	D	R	R
CHY061	S2	C	R	R
CHY060	S3	E	S	S
CHY059	S4	E	S	S
CHY058	S3	D	S	S
CHY057	S2	C	R	R
CHY055	S3	E	S	R
CHY054	S3	E	R	S
CHY052	S2	C	R	R
CHY050	S2	C	R	R
CHY047	S3	D	S	R
CHY046	S2	C	R	S
CHY044	S4	E	S	S
CHY042	S2	?	S	S
CHY041	S2	D	R	S
CHY039	S3	E	S	S
CHY036	S3	D	R	S
CHY035	S2	D	R	S
CHY034	S2	D	R	S
CHY023	S3	D	S	S
CHY022	S2	C	R	R
CHY019	S2	D	R	R
CHY017	S3	E	S	S
CHY016	S3	E	S	R
CHY015	S4	D	S	R
CHY014	S2	D	R	R
CHY012	S4	E	S	S
CHY010	S2	D	R	R
CHY008	S3	E	S	R
CHY006	S2	D	R	S

Note: RSS is Response Spectral Shape and HVSR is Horizontal to Vertical Spectral Ratio. The RSS classification is our recommendation.

**Appendix B: Site classification for 420 sites in Taiwan**

Sites classified as soil (248 sites)	Sites classified as rock (172 sites)
CHK; CHY002; CHY008; CHY012; CHY015; CHY016; CHY017; CHY023; CHY024; CHY025; CHY026; CHY032; CHY033; CHY039; CHY042; CHY044; CHY047; CHY055; CHY058; CHY059; CHY060; CHY066; CHY067; CHY069; CHY070; CHY071; CHY076; CHY078; CHY090; CHY092; CHY096; CHY099; CHY100; CHY101; CHY104; CHY116; HEN; HSN; HWA003; HWA007; HWA011; HWA012; HWA013; HWA014; HWA015; HWA016; HWA017; HWA019; HWA028; HWA029; HWA031; HWA036; HWA041; HWA054; ILA002; ILA003; ILA004; ILA005; ILA006; ILA007; ILA012; ILA013; ILA016; ILA021; ILA024; ILA027; ILA030; ILA032; ILA035; ILA036; ILA037; ILA039; ILA041; ILA042; ILA044; ILA046; ILA048; ILA049; ILA051; ILA054; ILA055; ILA056; ILA061; ILA064; KAU003; KAU006; KAU007; KAU008; KAU010; KAU011; KAU012; KAU015; KAU018; KAU020; KAU022; KAU030; KAU032; KAU033; KAU034; KAU037; KAU038; KAU039; KAU043; KAU044; KAU046; KAU048; KAU051; KAU052; KAU057; KAU058; KAU062; KAU063; KAU064; KAU066; KAU073; KAU074; KAU075; KAU081; KAU082; KAU083; KAU086; KAU087; KAU088; SGL; TAI1; TAP; TAP003; TAP005; TAP006; TAP007; TAP008; TAP010; TAP012; TAP013; TAP014; TAP017; TAP020; TAP021; TAP024; TAP026; TAP028; TAP032; TAP036; TAP041; TAP042; TAP046; TAP049; TAP060; TAP065; TAP066; TAP069; TAP075; TAP077; TAP078; TAP079; TAP081; TAP083; TAP084; TAP087; TAP090; TAP094; TAP095; TAP097; TAP098; TAP100; TAW; TCU003; TCU006; TCU007; TCU008; TCU009; TCU010; TCU011; TCU015; TCU017; TCU031; TCU033; TCU036; TCU038; TCU039; TCU040; TCU048; TCU050; TCU051; TCU052; TCU054; TCU055; TCU056; TCU059; TCU060; TCU061; TCU063; TCU064; TCU067; TCU068; TCU070; TCU075; TCU081; TCU082; TCU092; TCU094; TCU096; TCU101; TCU102; TCU103; TCU106; TCU107; TCU109; TCU110; TCU111; TCU112; TCU116; TCU117; TCU118; TCU120; TCU123; TCU128; TCU136; TCU141; TCU147; TTN; TTN001; TTN003; TTN004; TTN005; TTN006; TTN007; TTN008; TTN009; TTN010; TTN012; TTN013; TTN014; TTN015; TTN016; TTN022; TTN023; TTN027; TTN032; TTN033; TTN036; TTN042; TTN045; TTN047; TTN048; WK; WSF; WTC.	ALS; CHY004; CHY006; CHY010; CHY014; CHY019; CHY022; CHY027; CHY028; CHY029; CHY034; CHY035; CHY036; CHY041; CHY046; CHY050; CHY052; CHY054; CHY057; CHY061; CHY062; CHY063; CHY065; CHY074; CHY079; CHY080; CHY081; CHY082; CHY086; CHY087; CHY088; CHY093; CHY094; CHY102; CHY107; CHY109; CHY110; ENA; ESL; HWA; HWA002; HWA005; HWA006; HWA009; HWA020; HWA022; HWA023; HWA024; HWA025; HWA026; HWA027; HWA030; HWA032; HWA033; HWA034; HWA035; HWA037; HWA038; HWA039; HWA043; HWA044; HWA045; HWA046; HWA048; HWA049; HWA050; HWA051; HWA053; HWA055; HWA056; HWA057; HWA058; HWA059; HWA060; HWA2; ILA001; ILA008; ILA010; ILA014; ILA015; ILA031; ILA043; ILA050; ILA052; ILA059; ILA062; ILA063; ILA066; ILA067; KAU001; KAU040; KAU042; KAU047; KAU050; KAU054; KAU069; KAU077; KAU078; KAU085; NCU; NSK; NST; NSY; PNG; SSD; STY; TAP034; TAP035; TAP043; TAP047; TAP051; TAP052; TAP053; TAP059; TAP067; TAP072; TAP086; TAP103; TCU; TCU014; TCU018; TCU025; TCU026; TCU029; TCU034; TCU042; TCU045; TCU046; TCU047; TCU049; TCU053; TCU057; TCU065; TCU071; TCU072; TCU074; TCU076; TCU078; TCU079; TCU083; TCU084; TCU085; TCU087; TCU089; TCU095; TCU098; TCU100; TCU104; TCU105; TCU113; TCU115; TCU119; TCU122; TCU129; TCU138; TCU140; TCU145; TTN002; TTN018; TTN020; TTN024; TTN025; TTN026; TTN028; TTN031; TTN040; TTN041; TTN044; TTN046; TTN050; TTN051; WNT.